LWT - Food Science and Technology 144 (2021) 111222

Contents lists available at ScienceDirect

LWT

journal homepage: www.elsevier.com/locate/lwt

QSAR-based physicochemical properties of isothiocyanate antimicrobials against gram-negative and gram-positive bacteria

Silvia Andini [a,b], Carla Araya-Cloutier [a], Bianca Lay [a], Gijs Vreeke [a], Jos Hageman [c], Jean-Paul Vincken [a,*]

[a] Laboratory of Food Chemistry, Wageningen University, P.O. Box 17, 6700 AA, Wageningen, the Netherlands
[b] Department of Chemistry, Satya Wacana Christian University, Jalan Diponegoro 52-60, Salatiga, 50711, Indonesia
[c] Biometris, Applied Statistics, Wageningen University & Research, P.O. Box 16, 6700 AA, Wageningen, the Netherlands

ARTICLE INFO

Keywords:
Crucifer
Electrophile
Glucosinolate
Natural food preservative
Quantitative structure-activity relationship

ABSTRACT

Isothiocyanates (ITCs) derived from Brassicaceae are potential food preservatives. Their antimicrobial ac-tivity is strongly influenced by their subclass and side chain. This is the first quantitative structure-activity relationships (QSAR) study of ITCs as antibacterials. Twenty-six ITCs covering 9 subclasses were tested against *Escherichia coli* and *Bacillus cereus*. Minimum inhibitory concentration (MIC) and growth inhibitory response (GIR) were determined and used to develop QSAR models. MIC of the most active ITCs was 6.3–9.4 μg/mL. The QSAR models were validated with leave-one-out cross validation. The proposed models had a good fit (R^2_{adj} 0.86–0.93) and high internal predictive power (Q^2_{adj} 0.80–0.89). Partial charge, polarity, reactivity, and shape of ITCs were key physicochemical properties underlying antibacterial activity of ITCs. Furthermore, ITC compositions and antibacterial activity of *Sinapis alba*, *Brassica napus*, *B. juncea*, *B. oleracea*, and *Camelina sativa* extracts were determined, after myrosinase treatment. *B. oleracea* ITC-rich extract showed promising activity (MIC 750–1000 μg/mL) against both bacteria. *C. sativa* ITC-rich extract showed promising activity (MIC 188 μg/mL) against *B. cereus*. The QSAR models successfully predicted activity of the extracts based on ITC compositions. The models are useful to predict antibacterial activity of new ITCs and ITC-rich mixtures. Brassicaceae ITC-rich extracts are promising natural food preservatives.

1. Introduction

There is a continuous search for new safe natural compounds to prevent microbial growth in food products. This is along with consumers' concern about health-related risks of synthetic preservatives and with the increased antimicrobial persistence and resistance (Windels et al., 2019).

Structural diversity of plant-derived antimicrobial compounds is enormous. Among them, ITCs have been recognized as potential candidates for new antimicrobial compounds with broad spectrum of activity (Andini, Araya-Cloutier, Waardenburg, den Besten, & Vincken, 2020). They are naturally obtained from hydrolysis of glucosinolates (GSLs) by myrosinase in the Brassicaceae family (Blažević et al., 2020). Activity of ITCs is highly influenced by their structure. Previously, we showed some structure-activity relationships (SAR) of ITCs from aliphatic and benzenic classes with a diverse set of compounds (different side chain motifs and lengths) (Andini, Araya-Cloutier, Waardenburg, den Besten, & Vincken, 2020). Nevertheless, our previous study comprised a relatively small dataset of ITCs ($n = 10$), with 2 representatives per subclass. Thus, establishment of appropriate quantitative SAR (QSAR) was not possible (Hawkins, 2004). Up to date there is no QSAR study on ITCs as antimicrobials.

The aim of this study was to reveal the key physicochemical properties of ITCs underlying their antimicrobial activity against $Gram^-$ and $Gram^+$ bacteria by using a QSAR approach. Twenty-six ITCs, belonging to 9 subclasses (Fig. 1), were studied for this aim. Four new subclasses were investigated in this current study compared with our previous one (Andini, Araya-Cloutier, Waardenburg, et al., 2020): alkyl ITC, alkyl bifunctional ITC (i.e. alkyl diITC), *x*-(methylsulfinyl)alkenyl ITC, and *x*-(methylsulfonyl)benzenic ITC. *E. coli* and *B. cereus* were chosen as a representative of $Gram^-$ and $Gram^+$ bacteria, respectively, because of their highest susceptibility towards ITCs among previously tested bacterial species (Andini, Araya-Cloutier, Waardenburg, et al., 2020). The majority of these 26 ITCs has never been tested before against these

* Corresponding author.
E-mail address: jean-paul.vincken@wur.nl (J.-P. Vincken).

https://doi.org/10.1016/j.lwt.2021.111222
Received 28 October 2020; Received in revised form 8 February 2021; Accepted 27 February 2021
Available online 9 March 2021

bacterial species. Furthermore, ITC-rich extracts obtained from hydrolysis of GSL-rich extracts from widely consumed Brassicaceae seeds, namely *Sinapis alba*, *Brassica napus*, *B. juncea*, *B. oleracea*, and *Camelina sativa*, were tested for their antimicrobial activity and used for confirming the prediction ability of the developed QSAR models.

2. Materials and methods

2.1. Standard ITCs and GSLs, other chemicals, and growth media

Structures of 28 ITCs involved in this study are displayed in Fig. 1. Twenty-six ITC standards were available. Allyl ITC (AITC), 3-butenyl ITC (BuITC), 4-pentenyl ITC (PeITC), propyl ITC (PITC), 3-(methylthio)propyl ITC (3-MTITC), benzyl ITC (BITC), and phenethyl ITC (PhEITC) were from Sigma-Aldrich Chemie B.V. (St. Louis, Missouri, U.S.A.). 3-(Methylsulfinyl) propyl ITC (3-MSITC), 4-(methylsulfinyl)butyl ITC (4-MSITC), 5-(methylsulfinyl)pentyl ITC (5-MSITC), 6-(methylsulfinyl)hexyl ITC (6-MSITC), 8-(methylsulfinyl)octyl ITC (8-MSITC), 9-(methylsulfinyl)nonyl ITC (9-MSITC), 4-(methylsulfinyl)-3-butenyl ITC (4-MS-3-en-ITC), 3-(methylsulfonyl)propyl ITC (3-MSoITC), 4-(methylsulfonyl)butyl ITC (4-MSoITC), 5-(methylsulfonyl)pentyl ITC (5-MSoITC), 6-(methylsulfonyl)hexyl ITC (6-MSoITC), 8-(methylsulfonyl)octyl ITC (8-MSoITC), 9-(methylsulfonyl) nonyl ITC (9-MSoITC), 4-(methylthio)butyl ITC (4-MTITC), 5-(methylthio) pentyl ITC (5-MTITC), 6-(methylthio)hexyl isothiocyanate (6-MTITC), and 9-(methylthio)nonyl ITC (9-MTITC) were from Abcam (Cambridge, UK). 1,3-Propylene diisothiocyanate (P-DiITC) and *p*-(methylsulfonyl)phenyl ITC (*p*-MSoPhITC) were from ABCR GmbH (Karlsruhe, Germany).

GSLs (the names of the side chains are abbreviated according to ITCs', unless otherwise stated): 3-MSGSL, 4-MSGSL, 4-MTGSL, 5-MTGSL, AGSL, BGSL, BuGSL, indol-3-ylmethyl GSL (I3MGSL), PeGSL, PhEGSL, *p*-hydroxy-benzyl GSL (*p*-OH-BGSL), and (*R*)-2-hydroxy-3-butenyl GSL ((*R*)-2-OH-BuGSL) were from Phytolab GmbH & Co (Vestenbergsgreuth, Germany).

Ampicillin sodium and myrosinase (EC 3.2.1.147) were from Sigma-Aldrich Chemie B.V. Dimethyl sulfoxide (DMSO) was from Ducheda Biochemie (Haarlem, the Netherlands). *N*-acetyl-L-cysteine (NAC) was from Cayman Chemicals (Michigan, USA). Ultra-high performance liquid chromatography (UHPLC) grade isopropanol (IPA), formic acid (FA) 0.1% (v/v) in water, and FA 0.1% (v/v) in acetonitrile (ACN) were from Biosolve B.V. (Valkenswaard, The Netherlands). High purity water was produced using a Milli-Q A10 Gradient system (18.2 MΩ cm, 3 μg/kg total organic carbon) (Merck Millipore, Darmstadt, Germany).

Growth media: tryptone soya agar (TSA) and tryptone soya broth (TSB) were from Oxoid Limited (Hampshire, U.K.); bacteriological agar from VWR International B.V. (Valkenswaard, The Netherlands); bacto brain heart infusion from Becton, Dickinson and Company (Franklin Lakes, NJ, U.S.A.). Peptone physiological salt solution (PPS) was from Tritium Microbiologie (Eindhoven, The Netherlands).

2.2. Microbial cultures

E. coli K12 and *B. cereus* ATCC 14579 were kindly provided by the laboratory of Food Microbiology, Wageningen University, The Netherlands.

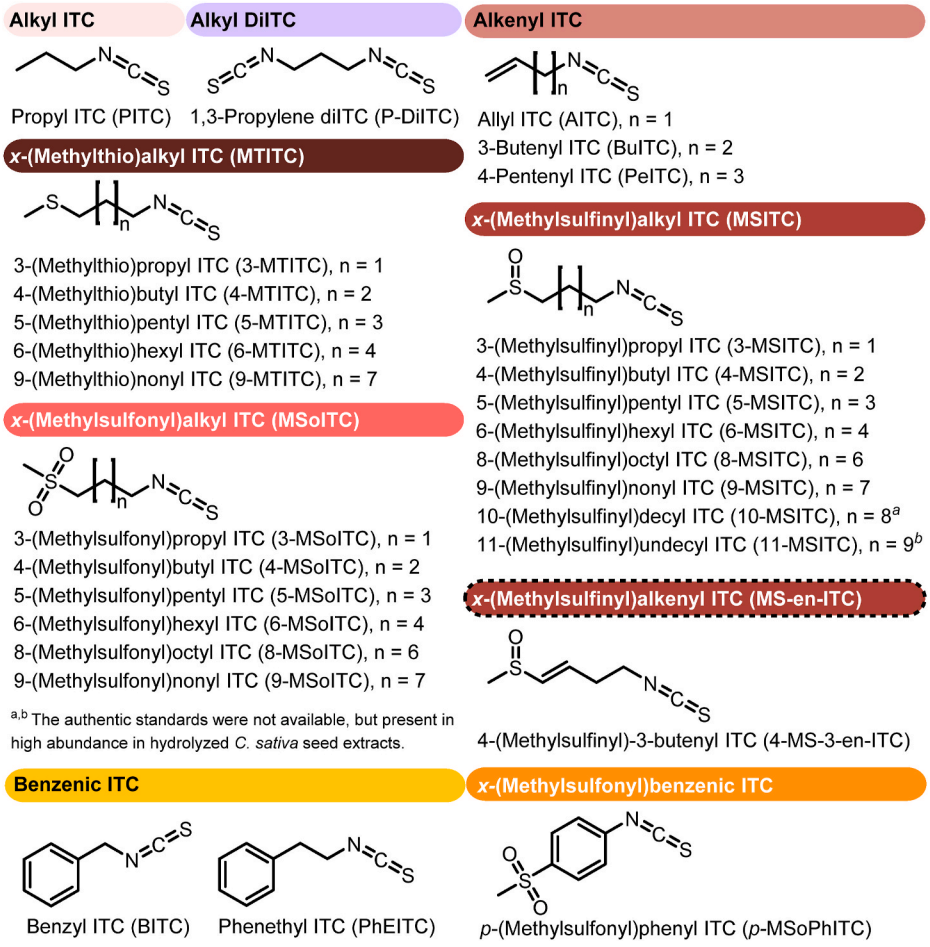

Fig. 1. ITCs used in this study. Subclasses are differentiated by colors. (For interpretation of the references to color in this figure legend, the reader is referred to the Web version of this article.)

2.3. Plant materials

Seeds of *S. alba* (yellow mustard 'Emergo', 393,810), *B. napus* ('Helga', 392,600), *B. juncea* var. rugosa rugosa (Chinese mustard/ amsoi, 160,400), *B. oleracea* var. botrytis subvar. Cymosa (broccoli, 145,100), and *C. sativa* (German sesame, 390,900) were from Vreeken's Zaden (Dordrecht, The Netherlands, https://www.vreeken.nl/). *B. juncea* var. rugosa rugosa and *B. oleracea* var. botrytis subvar. Cymosa are mentioned as *B. juncea* and *B. oleracea*, respectively, in the following text.

2.4. Extraction of Brassicaceae seeds

Five seed extracts were obtained through methanol extraction, performed in a Speed Extractor (E−916; Büchi, Flawil, Switzerland) (Andini, Dekker, Gruppen, Araya-Cloutier, & Vincken, 2019). Dried extracts were stored at −20 °C. Stock extracts (10 mg/mL) were resolubilized in 10% (v/v) DMSO in phosphate buffer pH 7.0.

2.5. Enzymatic hydrolysis of extracts

Extracts (2 mg/mL) were mixed with commercial myrosinase (0.05 U/mL, 1 U was defined as the amount of enzyme that releases 1 μmol glucose per min with AGSL as the substrate, at 25 °C, pH 6.0). Hydrolysis was performed at 50 °C, pH 7.0 for 4 h, in two ways: (i) in the presence of NAC for the LC-MS analysis (Andini, Araya-Cloutier, Sanders, & Vincken, 2020), (ii) in the absence of NAC for the antibacterial assay. As a control, the non-hydrolyzed extracts were prepared in the same way, only that the myrosinase solution was replaced by buffer pH 7.0.

2.6. RP-UHPLC-ESI-MS^n analysis of (hydrolyzed) Brassicaceae seed extracts

Analysis of GSLs and ITCs was performed according to (Andini, Araya-Cloutier, Sanders, & Vincken, 2020), in an Accela UHPLC system (Thermo Scientific, San Jose, CA, USA) coupled to an LTQ Velos electrospray ionization (ESI) ion trap mass spectrometer (MS) (Thermo Scientific). FA 0.1% in water (eluent A) and FA 0.1% in ACN (eluent B) were used at 300 μL/min. The elution gradient was 0–6.7 min, isocratic on 0% (v/v) B; 6.7–12.5 min, linear gradient to 8% B; 12.5–24.2 min, linear gradient to 16% B; 24.2–41.8 min, linear gradient to 40% B; 41.8–43.5 min, linear gradient to 100% B; 43.5–50.5 min, isocratic on 100% B; 50.5–52 min, linear gradient to 0% B; 52–59 min, isocratic on 0% B. (Tentative) annotation and quantification of GSLs and ITCs (as NAC-ITCs) were based on UV and MS spectra, performed in Xcalibur (v.2.2, Thermo Scientific) (Andini et al., 2019, 2020a). Calibration curves of GSLs and ITCs were within 2.5–50 μmol/L. GSLs and ITCs without authentic standards were quantified based on calibration curves of those with the most similar structure, and corrected by the molecular weight.

2.7. Antibacterial assay

Antibacterial activity of ITCs was determined by following the broth-microdilution procedure (Andini, Araya-Cloutier, Waardenburg, et al., 2020). In short, the inoculum at 3.7 ± 0.3 log_{10} CFU/mL was prepared in TSB (specifically 10× diluted TSB). Stock solutions of standard ITCs were prepared at 10 mg/mL in DMSO. Final concentrations of ITCs varied from 3.0 to 200.0 μg/mL (DMSO 2% (v/v) max.). Positive control (ampicillin 1.5 μg/mL for *E. coli*, 15 μg/mL for *B. cereus*), negative control (the inoculum and liquid medium with DMSO 2%), and blank (the liquid medium without any inoculum and antibacterial agent) were included in every assay. The microbial growth was monitored spectrophotometrically at OD_{600} (SpectraMax iD3, Molecular Devices, U.S.A.) every 10 min for 24 h at 30 °C for *B. cereus* or 37 °C for *E. coli*, with a constant periodic shaking. Antibacterial activity of ITCs was evaluated in minimum 3 independent biological repetitions, each performed in duplicate.

Time-to-detection (TTD) of growth was determined when OD increased 0.05 units (Aryani, den Besten, Hazeleger, & Zwietering, 2015). When the increase was not observed after 24 h, cell viability was checked by plate counting to determine minimum inhibitory concentration (MIC) and minimum bactericidal concentration (MBC) (Araya-Cloutier et al., 2018). Growth inhibitory response (GIR, h $mmol^{-1}$ L) was determined as the growth inhibitory effect (h) caused by an ITC per molar-based concentration (mmol/L) (Figure S1).

All procedures were also applied for testing the antibacterial activity of (hydrolyzed) Brassicaceae seed extracts. (Hydrolyzed) extracts were tested up to 1000 μg/mL. Furthermore, to demonstrate that the antibacterial activity of the hydrolyzed extract was mainly due to ITCs and that there was no interaction between ITCs in the extract, a mixture with similar ITC composition as was in the extract was prepared. This mixture is called as the model extract. The antibacterial activity of the (hydrolyzed) extracts and the model extract was evaluated in 3 independent biological repetitions, each performed in duplicate. GIR of the hydrolyzed extracts and the model extract was calculated based on total ITC concentration (mmol/L) in the mixture.

2.8. Time-kill kinetic assay

Time-kill kinetic curves were made of the most active ITCs at their MBC against *E. coli* and *B. cereus* (Tsou, Hu, Yang, Yan, & Lin, 2019). Likewise, hydrolyzed *C. sativa* extract was also prepared. The bacterial inoculum was prepared in a similar way as described previously (section **2.7**). Bacterial inoculum was incubated with ITCs or hydrolyzed *C. sativa* extract for 24 h at 30 °C or 37 °C in a shaking incubator at 800 rpm. At time points 1, 2, 3, 4, 6, and 24 h, the aliquots were inoculated aseptically onto TSA plates to check the cell viability. Positive control, negative control, and blank were included. The assay was performed in 2 independent biological repetitions, each performed in duplicate.

2.9. QSAR modeling

Molecular Operating Environment (MOE) software (version 2018.0101, Chemical Computing Group, Montreal, QC, Canada) was used for *in silico* modeling of the antibacterial activity of 26 ITCs against *E. coli* and *B. cereus*. Molecular structures of ITCs were inserted into a database by use of the canonical Simplified Molecular Input Line Entry System (SMILES) obtained from PubChem database (Gindulyte et al., 2015). When the SMILES of an ITC was not available in PubChem, the ITC was drawn in ChemDraw 18.0 (PerkinElmer Informatics, Inc., Waltham, MA, U.S.A.) and then inserted into MOE.

ITC molecules were energy minimized by using the molecular orbital package (MOPAC) PM3 at a root mean square (RMS) gradient of 0.01 kcal/mol/$Å^2$. Furthermore, a conformational search was performed by using LowModeMD method with a rejection limit of 50, an iteration limit of 10,000, an RMS gradient of 0.1 kcal/mol/$Å^2$, an MM iteration limit of 500, an RMSD limit of 0.25, and a conformation limit of 5. The conformer with the lowest energy was chosen.

Afterwards, 2D and 3D molecular descriptors were calculated. In addition to the descriptors available at MOE, the partial charges on the carbon atom and the nitrogen atom of the –N═C═S group and the global electrophilicity (ω^o) were calculated using MOE (full list of used descriptors shown in Table S1). Global electrophilicity, or electrophilicity from this point onwards, was calculated with the following formulae (Parr, Szentpály, & Liu, 1999). The descriptor database was curated by eliminating highly inter-correlated descriptors ($R^2 \geq 0.95$) and constant descriptors.

$$hardness,\ \eta = \frac{E_{LUMO} - E_{HOMO}}{2} \quad (1)$$

$$chemical\ potential,\ \mu = \frac{E_{HOMO} + E_{LUMO}}{2} \quad (2)$$

$$global\ electrophilicity,\ \omega^{o} = \frac{\mu^2}{2\eta} \quad (3)$$

MIC, as pMIC (i.e. $-log_{10}$MIC, mmol/L), was used in previous QSAR studies of other antimicrobial compounds (Araya-Cloutier et al., 2018; Dolezal et al., 2016). However, not all tested ITCs had a defined MIC up to the highest tested concentration (Andini, Araya-Cloutier, Waardenburg, et al., 2020). Meanwhile, delayed bacterial growth was observed in the presence of ITCs. Therefore, in this QSAR study, antimicrobial activity of ITCs was also quantified as GIR. GIR, as p'GIR (i.e. log_{10}GIR, h mmol^{-1} L), allows us to input the activity of every ITC transparently (i.e. without imputation) to the QSAR modeling. In this current QSAR study, the antibacterial activity of ITCs against *E. coli* and *B. cereus* was separately modeled using pMIC and p'GIR. ITCs with no defined MIC (i.e. MIC >200.0 μg/mL) were included in the modeling by imputing a MIC 400 μg/mL (i.e. next 2-fold concentration to be tested) (Araya-Cloutier et al., 2018). GIR and MIC values were transformed to a logarithmic scale to improve the normality of data distribution and the interpretation of the antibacterial activity (i.e. higher pMIC or p'GIR for higher antibacterial activity and vice versa). Because of the size of the available dataset (26 ITCs), splitting into training and test sets was not recommended (models may not contain all the relevant structural information of the whole dataset) (Gramatica, 2007; Tropsha, 2010). Thus, models were validated using a leave-one-out cross validation (LOO-CV) procedure (expressed as a Q^2 value).

A genetic algorithm (GA) was used to select a small subset of descriptors best able to predict the antibacterial activities (pMIC or p'GIR) using multiple linear regression. The GA approach has been adapted from previous studies (Araya-Cloutier et al., 2018; de Bruijn, Hageman, Araya-Cloutier, Gruppen, & Vincken, 2018). Q^2 values were used as indicators of the fitness of selected descriptors (Hageman et al., 2017) and maximized by the GA. To exclude lucky or unlucky GA runs, every run was repeated 12 times with different starting seeds. Combinations of descriptors with a variance inflation factor (VIF) > 5, indicating a strong inter-correlation, were effectively removed from the GA population by penalizing the fitness during the GA run. GA parameters were optimized using a full factorial experimental design and were found to be: population size = 150, cross-over rate = 0.8, mutation rate = 0.3. The maximum number of iterations was set to 300 and elitism set to 8. The number of descriptors to be selected during a GA run was varied between 2 and 5, since the ratio between number of compounds and number of descriptors in a model should be ≥ 5 (Xu & Zhang, 2001).

Furthermore, the applicability domain was determined with the Williams plot (Gramatica, 2013). In this plot, ITCs with large standardized residuals and/or large leverages can be tracked down, indicating ill-fitting or highly influential compounds in the model, and were considered as outliers. Lastly, to further minimize the risk of overfitting, a permutation test was performed by repeating 100 times the exact procedure but with a permuted pMIC or p'GIR response variable, effectively modeling random data. Using the 100 permuted Q^2 values, a *p*-value for the true GA run can be calculated, indicating if this result could have occurred by chance.

The internal prediction ability of the final chosen model should have a $Q^2 > 0.5$ and $R^2 > 0.7$. Furthermore, the difference between R^2 and R_0^2 (R^2 of the intercept) aimed to be minimum (<0.1) (Tropsha, 2010). The modified R^2 metric (i.e. $\overline{R_m^2}$) was calculated to fortify the statistical internal predictivity of the model (Figure S2) (Roy et al., 2013).

3. Results

Table 1 shows the antimicrobial activity expressed as MIC, MBC, and GIR of each ITC against each bacterium. A good antimicrobial activity in this study was defined as MIC ≤25 μg/mL and GIR ≥114 h mmol^{-1} L (the minimum GIR associated with a MIC of 25 μg/mL was 114.7 ± 23.5 h mmol^{-1} L). P-DiITC, an alkyl ITC with bifunctional –N=C=S groups, had the highest activity against *E. coli* (MIC 9.4 μg/mL, GIR 237.8 h mmol^{-1} L) and against *B. cereus* (MIC 6.3 μg/mL, GIR 541.7 h mmol^{-1} L). MBC of P-DiITC was 12.5 μg/mL for each bacterium. In contrast, PITC, the monofunctional analogue, had poor activity (MIC > 200.0 μg/mL, GIR ≤ 3.0 h mmol^{-1} L).

All good antibacterial ITCs showed bactericidal effects in the range of 12.5–100.0 μg/mL against *E. coli* and 12.5–50.0 μg/mL against *B. cereus*. Killing kinetic studies (Figure S3) showed that antibacterial ITCs mainly inhibited bacterial growth during the first 6 h and that after 24 h more than 99.9% of cells were inactivated.

3.1. Structure-activity relationship

3.1.1. Effect of ITC class

Good antibacterial ITCs belonged only to the aliphatic class. Subclasses alkyl bifunctional, *x*-(methylsulfinyl)alkyl (MSITC), and *x*-(methylsulfonyl)alkyl (MSoITC) were the most active ones. In contrast, the benzenic class showed moderate to low activity (MIC ≥ 100 μg/mL and GIR ≤ 27 h mmol^{-1} L).

3.1.2. Effect of oxidation of sulfur substituent

ITCs from subclasses *x*-(methylthio)alkyl ITC (MTITC), MSITC, and MSoITC share similar structure but have an increasing order in the oxidation state of the sulfur substituent. The lowest MIC obtained for these three subclasses was 150.0 μg/mL (each bacterium), 25.0/15.0 μg/mL (*E. coli*/*B. cereus*), and 25.0/9.4 μg/mL (*E. coli*/*B. cereus*), respectively. In line with a previous study, an increased oxidation state of the sulfur substituent in the side chain of ITCs improved the antimicrobial activity (Andini, Araya-Cloutier, Waardenburg, et al., 2020).

3.1.3. Effect of chain length

3-MTITC (MIC 150.0 μg/mL) had higher antimicrobial activity against each bacterium than the other MTITCs with longer chain length (*C4* to *C9*). Meanwhile, MSITCs and MSoITCs exerted different trend of activity per bacterium. Against *E. coli*, the activity of MSITCs increased with decreasing chain length from *C9* to *C3* (MIC from ≥200.0 μg/mL to 25.0 μg/mL). Against *B. cereus*, the activity of MSITCs tended to increase with increasing chain length from *C5/C6* to *C9* (MIC from 50.0 μg/mL to 15.0 μg/mL). The trends of MSoITCs were comparable to those of MSITCs against *E. coli*. Against *B. cereus*, MSoITCs *C3–C9* were considered to have good activity (MIC ≤ 25 μg/mL), except the *C6* analogue (moderate activity, MIC 37.5 μg/mL).

3.2. Antibacterial activity of ITC-rich extracts and their ITC compositions

ITC-rich extracts were obtained from Brassicaceae extracts, rich in GSLs, treated with commercial myrosinase. The detailed information on the compositions of GSLs and ITCs in the extracts before and after hydrolysis are available in Supporting Information, including Figure S4 and Tables S2–S4. The overview of ITC compositions of the myrosinase-treated extracts at 1.0 mg/mL is presented in Fig. 2.

B. oleracea ITC-rich extract had antibacterial activity against *E. coli* (MIC 1000.0 μg/mL, corresponding to an ITC concentration of 53.5 μg/mL or 324.1 μmol/L, GIR 106.9 h mmol^{-1} L) and *B. cereus* (MIC 750.0 μg/mL corresponding to an ITC concentration of 40.1 μg/mL or 243.1 μmol/L, GIR 76.2 h mmol^{-1} L) (Table 1). This extract was rich in short-chained (*C3* and *C4*) MSITCs (252.0 μmol/L) and MTITCs (59.2 μmol/L) (Fig. 2, Table S4). In contrast, the *C. sativa* ITC-rich extract had good activity only against *B. cereus* (MIC 188.0 μg/mL, corresponding to an ITC concentration of 24.3 μg/mL or 93.5 μmol/L, GIR 155.4 h mmol^{-1} L) but not against *E. coli* (MIC > 1000.0 μg/mL, GIR 3.1 h mmol^{-1} L). *C. sativa* ITC-rich extract was rich in the long-chained (*C9–C11*) MSITCs (496.3 μmol/L) (Table S4). *B. juncea* ITC-rich extract was mainly composed of alkenyl ITCs (439.7 μmol/L) and had poor activity against

Table 1
Antibacterial activity of ITCs, ITC-rich Brassicaceae extracts, and the model *B. oleracea* ITC-rich extract.[a].

No.	ITC[b]	*E. coli*			*B. cereus*		
		MIC	MBC	GIR	MIC	MBC	GIR
Pure ITC							
1	PITC	>200.0	>200.0	2.9 ± 2.7[c]	>200.0	>200.0	0.5 ± 0.2
2	P-DiITC	9.4	12.5	237.8 ± 6.9	6.3	12.5	541.7 ± 192.6
3	AITC	>200	>200.0	3.2 ± 0.3	>200.0	>200.0	3.0 ± 2.0
4	BuITC	>200	>200.0	4.4 ± 2.6	>200.0	>200.0	1.3 ± 1.4
5	PeITC	>200	>200.0	1.6 ± 1.2	>200.0	>200.0	0.9 ± 0.2
6	3-MTITC	150.0	200.0	19.6 ± 4.5	150.0	200.0	24.5 ± 5.5
7	4-MTITC	>200.0	>200.0	10.1 ± 3.4	200.0	>200.0	14.8 ± 0.5
8	5-MTITC	>200.0	>200.0	5.2 ± 2.4	200.0	>200.0	15.9 ± 1.1
9	6-MTITC	>200.0	>200.0	2.1 ± 0.9	>200.0	>200.0	19.1 ± 5.9
10	9-MTITC	>200.0	>200.0	1.3 ± 0.5	>200.0	>200.0	9.5 ± 8.5
11	3-MSITC	25.0	50.0	140.7 ± 37.1	25.0	50.0	114.7 ± 23.5
12	4-MSITC	50.0	200.0	84.2 ± 28.2	25.0	50.0	115.9 ± 11.2
13	5-MSITC	50.0	200.0	68.7 ± 3.4	50.0	100.0	73.1 ± 2.7
14	6-MSITC	100.0	200.0	35.1 ± 11.5	50.0	75.0	96.9 ± 26.9
15	8-MSITC	>200.0	>200.0	16.1 ± 0.6	25.0	50.0	177.9 ± 0.3
16	9-MSITC	200.0	>200.0	12.2 ± 7.9	15.0	25.0	356.7 ± 9.3
17	4-MS-3-en-ITC	25.0	100.0	208.5 ± 65.1	25.0	50.0	121.6 ± 13.6
18	3-MSoITC	25.0	50.0	247.1 ± 31.0	25.0	50.0	196.2 ± 73.1
19	4-MSoITC	25.0	100.0	144.0 ± 6.0	25.0	50.0	184.2 ± 64.1
20	5-MSoITC	75.0	150.0	79.7 ± 0.3	25.0	50.0	157.0 ± 0.7
21	6-MSoITC	100.0	150.0	46.6 ± 24.7	37.5	50.0	124.9 ± 33.9
22	8-MSoITC	>200.0	>200.0	19.0 ± 2.8	12.5	25.0	212.8 ± 0.2
23	9-MSoITC	>200.0	>200.0	2.2 ± 1.5	9.4	12.5	624.1 ± 154.8
24	BITC	150.0	200.0	18.2 ± 5.4	100.0	150.0	27.1 ± 0.8
25	PhEITC	>200.0	>200.0	7.8 ± 2.7	150.0	200.0	20.5 ± 1.4
26	*p*-MSoPhITC	>200.0	>200.0	7.7 ± 2.2	>200.0	>200.0	16.7 ± 3.8
ITC-rich Brassicaceae seed extracts							
Camelina sativa (*Cs*)		>1000.0[d]	>1000.0	3.1 ± 1.7[e]	188.0	375.0	155.4 ± 8.8
Brassica oleracea (*Bo*)		1000.0	>1000.0	106.9 ± 19.9	750.0	1000.0	76.2 ± 27.1
Brassica juncea (*Bj*)		>1000.0	>1000.0	1.5 ± 1.3	>1000.0	>1000.0	0.3 ± 0.4
Brassica napus (*Bn*)		>1000.0	>1000.0	3.3 ± 2.0	>1000.0	>1000.0	2.2 ± 2.1
Sinapis alba (*Sa*)		>1000.0	>1000.0	3.0 ± 3.6	>1000.0	>1000.0	3.7 ± 2.6
Model *Bo* extract[f]		1000.0	>1000.0	109.0 ± 2.2	1000.0	>1000.0	56.2 ± 3.5

[a] The antibacterial activity is expressed as minimum inhibitory concentration (MIC, μg/mL), minimum bactericidal concentration (MBC, μg/mL), and growth inhibitory response (GIR, h mmol^{-1} L).
[b] PITC, P-DiITC, and *p*-MSoPhITC are non-plant derived ITCs. The GSL precursor of 5-MSoITC can be biosynthetically formed in plants, but its presence has never been identified unambiguously (Blažević et al., 2020).
[c] GIR is displayed as the average and standard deviation from three to seven independent biological repetitions.
[d] MIC and MBC of the ITC-rich extracts and the model extract refer to the concentrations of extracts, and not to the concentration of ITCs. The highest concentration of the ITC-rich extracts in the assays was 1000.0 μg/mL.
[e] GIR of the ITC-rich extracts is expressed in h mmol^{-1} L based on the concentration of the 5 major ITCs present in the extracts.
[f] The model *C. sativa* ITC-rich extract could not be made due to lack of authentic standards of 10-MSITC and 11-MSITC.

each bacterium (MIC > 1000.0 μg/mL, GIR ≤ 1.5 h mmol^{-1} L). This was consistent with the results found for the pure alkenyl ITCs. These findings emphasize that ITC composition is more important than just ITC content for the antimicrobial activity of myrosinase-treated Brassicaceae extracts. The other two extracts from *S. alba* and *B. napus* contained less than 30 μmol/L ITCs (mainly composed of benzenic ITC and alkenyl ITC, respectively) and had poor activity against *E. coli* and *B. cereus* (MIC > 1000.0 μg/mL, GIR ≤ 3.7 h mmol^{-1} L).

3.3. QSAR modeling

In this study, 26 ITCs were used as training set to build QSAR models using pMIC (–log_{10}MIC, mmol/L) and p'GIR (log_{10}GIR, h mmol^{-1} L) as activity response variables. QSAR models were developed with up to 5 molecular descriptors (k = 2, 3, 4, 5) to prevent overfitting (Xu & Zhang, 2001) or having too complex models. For this, the selection of the number of descriptors was based on the internal predictive power (Q^2) (Figure S5) as well as on other criteria specified in Table S5 (de Bruijn et al., 2018). All developed QSAR models had a good fit ($R^2 \geq 0.75$, $R^2_{adj} \geq 0.73$, and $\overline{R^2_m} \geq 0.71$) and a good internal predictive power ($Q^2 \geq 0.68$, $Q^2_{adj} \geq 0.66$) (Table S5). Based on the number of descriptors, statistical performance, and outliers, the models with 4 descriptors (k = 4) were chosen for both bacteria (Table 2). Fig. 3A–D illustrate the good fit of the predicted values calculated by the chosen models to the observed values ($R^2 \geq 0.88$) and high internal prediction ability ($Q^2 \geq 0.83$). The permutation tests indicated that all the chosen models were significant (p-value < 0.001) (Figure S6). One structural outlier (high leverage value), i.e. *p*-MSoPhITC, was found for pMIC model for *B. cereus* (Figure S7).

3.3.1. QSAR models for E. coli

The pMIC model for *E. coli* (Table 2) indicated that the antibacterial activity of ITCs was positively correlated to topological polar surface area (*TPSA*), fractional charge-weighted negative surface area (*FCASA*–), and hydrophilic volume (*vsurf_W1*), but negatively correlated to fractional charge-weighted positive surface area (*FCASA*+). As one might expect that *FCASA*– and *FCASA*+ can be strongly inter-correlated, it is worth to note that the variance inflation factor (VIF) values of *FCASA*– and *FCASA*+ were low (<5), meaning no strong inter-correlation, and that their contribution to the prediction was significant (p-values < 0.05). The p'GIR model for *E. coli* indicated that the antibacterial activity of ITCs was positively correlated to electronic energy (*PM3_Eele*) and hydrophobic integy moment (*vsurf_ID6*), but negatively correlated to relative positive partial charge (*PEOE_RPC*+) and molecular shape specified by ratio of

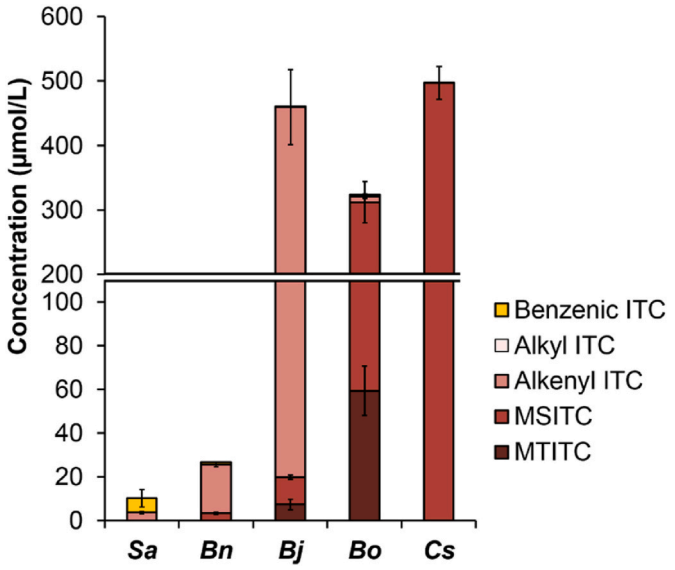

Fig. 2. Compositions of ITCs in 1 mg/mL myrosinase-treated seed extracts. *Sa*: *S. alba*, *Bn*: *B. napus*, *Bj*: *B. juncea*, *Bo*: *B. oleracea*, and *Cs*: *C. sativa*.

principal moment of inertia PMI2/PMI3 (*npr2*).

3.3.2. QSAR models for B. cereus

The pMIC model for *B. cereus* (Table 2) indicated that the antibacterial activity of ITCs was positively correlated to van der Waals surface area of partial positive charges (*PEOE_VSA+3*), hydrophilic-lipophilic balance (*vsurf_HL1*), and surface rugosity (roughness) (*vsurf_R*), but negatively correlated to global electrophilicity (*AM1_Electrophilicity*). Although one might expect that partial positive charge is related to electrophilicity (electron deficient property), the descriptors related to both had low VIF values (<5) and their contribution to the model was significant (p-values < 0.05). The p'GIR model for *B. cereus* indicated that the antibacterial activity of ITCs was positively correlated to molecular shape specified by principal moment of inertia PMI1/PMI3 (*npr1*), van der Waals surface area of partial negative charges (*PEOE_VSA-1*), and hydrophilic volume (*vsurf_W7*), but negatively correlated to hydrophilic integy moment (*vsurf_IW2*).

The QSAR models for *E. coli* and *B. cereus* indicated that molecular shape was more important for activity against *B. cereus* (*npr1*, p-value 4.3×10^{-9}) than against *E. coli* (*npr2*, p-value 2.5×10^{-5}), whereas reactivity was more important for activity against *E. coli* (*PM3_Eele*, p-value 1.6×10^{-8}) than against *B. cereus* (*AM1_Electrophilicity*, p-value 1.8×10^{-4}) (Tables S6-7).

3.3.3. Application of the QSAR models to predict the antibacterial activity of ITC-rich extracts

The developed QSAR models (Table 2) for *B. cereus* and *E. coli* were used to predict the antibacterial activity of the ITC-rich *C. sativa* and *B. oleracea* extracts. MICs of the extracts (µg/mL) presented in Table 1 were transformed to the total concentration (mmol/L) of ITCs in the extract. With the assumption that there was no interaction between ITCs in a mixture, the predicted antibacterial activity of ITC-rich extracts (pMIC and p'GIR) was calculated according to the contribution of each ITC in the extracts to the total antibacterial activity.

Fig. 3*E*–F shows that the predicted pMIC and p'GIR values of the ITC-rich *C. sativa* and *B. oleracea* extracts against *E. coli* and *B. cereus* matched to the respective observed values. In the case of *C. sativa* ITC-rich extract against *E. coli*, the negative predicted pMIC shown in Fig. 3E represents a MIC based on extract concentration of 3100 µg/mL, meaning that the predicted MIC was in line to the observed value (MIC > 1000 µg/mL). *C. sativa* ITC-rich extract contained abundantly two ITCs which were not in the training set, i.e. 10-MSITC and 11-MSITC, due to lack of standard compounds. The activity of 10-MSITC and 11-MSITC was predicted by the chosen models. Their predicted activity was in line with the observed and predicted activity of *C. sativa* ITC-rich extract, especially against *B. cereus*, i.e. the susceptible bacterium towards long-chained MSITCs.

The largest difference between the observed and the predicted values in Fig. 3*E*–F was perceived for pMIC of *B. oleracea* ITC-rich extract against *B. cereus* (0.668 vs 0.504, respectively, equaled to extract concentration of 750 µg/mL and 989 µg/mL, respectively). Other minor compounds present in the natural extract might contribute to the antimicrobial activity. Therefore, a model extract containing only ITCs, i.e. absent of other potential non-ITC compounds, was made to mimic the *B. oleracea* ITC-rich extract. MIC and GIR values of the model extract were comparable to those of the natural extract (Table 1). Only a slightly lower activity against *B. cereus* was found for the model extract (MIC 1000 µg/mL) in comparison with the natural extract (MIC 750 µg/mL), but similar to the predicted activity (MIC 989 µg/mL). This confirms that

Table 2
The chosen MLR regression models for predicting antibacterial activity of ITCs.

Bacteria	Activity parameter	Descriptor	Coefficient	Standard error	p-value	VIF
E. coli	pMIC	*TPSA*	0.030	0.0028	5.7×10^{-10}	2.24
		FCASA+	−1.000	0.105	4.9×10^{-9}	4.26
		FCASA-	0.819	0.127	2.2×10^{-6}	3.42
		Vsurf_W1	0.001	0.00038	0.045	1.74
		Intercept	−2.240	0.286	1.2×10^{-7}	–
	p'GIR	*PM3_Eele*	9.1×10^{-6}	1.0×10^{-6}	1.6×10^{-8}	3.38
		PEOE_RPC+	−11.170	1.449	1.5×10^{-7}	4.45
		npr2	−2.619	0.488	2.5×10^{-5}	1.42
		vsurf_ID6	0.274	0.138	0.061	1.59
		Intercept	7.276	0.613	8.8×10^{-11}	–
B. cereus	pMIC	*PEOE_VSA+3*	0.040	0.005	4.4×10^{-8}	2.98
		vsurf_HL1	6.413	0.826	1.3×10^{-7}	1.14
		vsurf_R	2.802	0.599	0.00013	1.40
		AM1_Electrophilicity	−0.985	0.217	0.00018	2.63
		Intercept	−3.831	0.844	0.00018	–
	p'GIR	*vsurf_IW2*	−1.386	0.128	7.6×10^{-11}	1.47
		npr1	2.622	0.274	4.3×10^{-9}	1.29
		PEOE_VSA-1	0.019	0.003	2.2×10^{-6}	1.54
		vsurf_W7	0.425	0.116	0.0033	1.24
		Intercept	1.401	0.154	9.5×10^{-9}	–

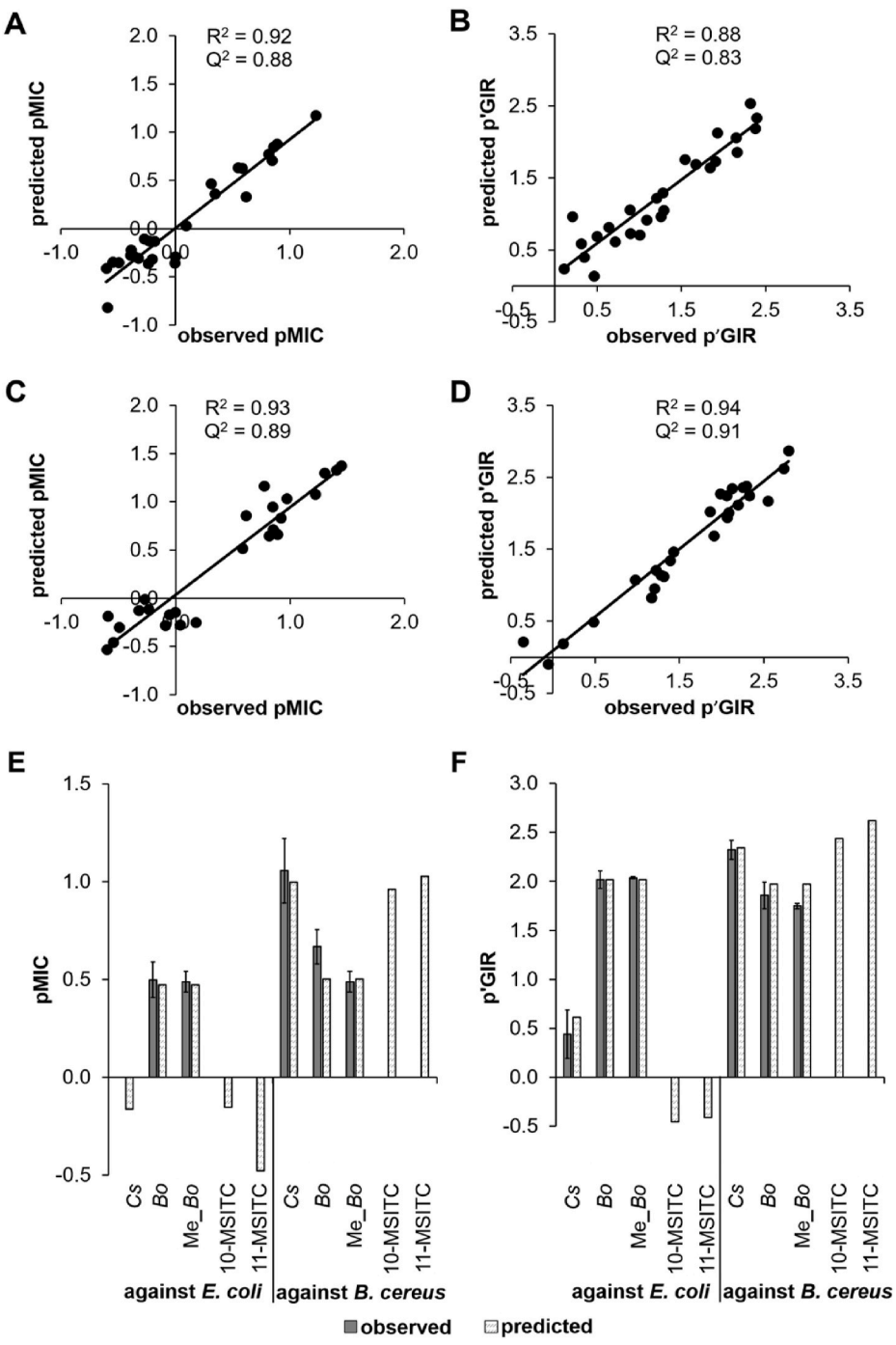

Fig. 3. Observed vs predicted antibacterial activity: pMIC and p'GIR of ITCs against *E. coli* (**A-B**) and against *B. cereus* (**C-D**), pMIC (**E**) and p'GIR (**F**) of ITC-rich mixtures and 10-MSITC and 11-MSITC against *E. coli* and *B. cereus*. *Cs*: *C. sativa* ITC-rich extract; *Bo*: *B. oleracea* ITC-rich extract; Me_*Bo*: model *B. oleracea* ITC-rich extract. The bar for observed pMIC of *Cs* against *E. coli* is absent due to MIC >1000.0 μg/mL (the highest tested extract concentration). The bars for observed pMIC and p'GIR of 10-MSITC and 11-MSITC against *E. coli* and *B. cereus* are absent due to lack of pure compounds for testing. The error bars in ***E*-F** represent the standard deviation with three biological independent repetitions.

the antibacterial activity of the ITC-rich natural extract was mainly due to the ITCs and that our QSAR models were able to predict well the activity of both natural and model ITC mixtures.

4. Discussion

4.1. The most important physicochemical properties of ITCs as antibacterials

Fig. 4A shows the most important classes of descriptors present in all statistically compliant models. Polarity, partial charge, reactivity, and molecular shape were important physicochemical properties of ITCs as antibacterials.

4.1.1. The importance of partial charge

Electrostatic surface maps of representative good and poor antibacterial ITCs are depicted in Fig. 4B (red-blue surface). It demonstrates that ITCs with strong electrostatic regions (e.g. 3-MSITC, 3-MSoITC, 9-MSoITC) have antibacterial activity, either against both bacteria or against Gram^{+} *B. cereus*, depending on the chain length. In contrast, ITCs without strong electrostatic regions (e.g. 9-MTITC, PITC) have no antibacterial activity, except the bifunctional ITC (section **4.2**). Partial charge might be an importance in influencing the interaction of the molecules with cell wall components (Lambert, 2002; Richter et al., 2017).

4.1.2. The importance of polarity

Most active ITCs had distinct hydrophilic and hydrophobic regions

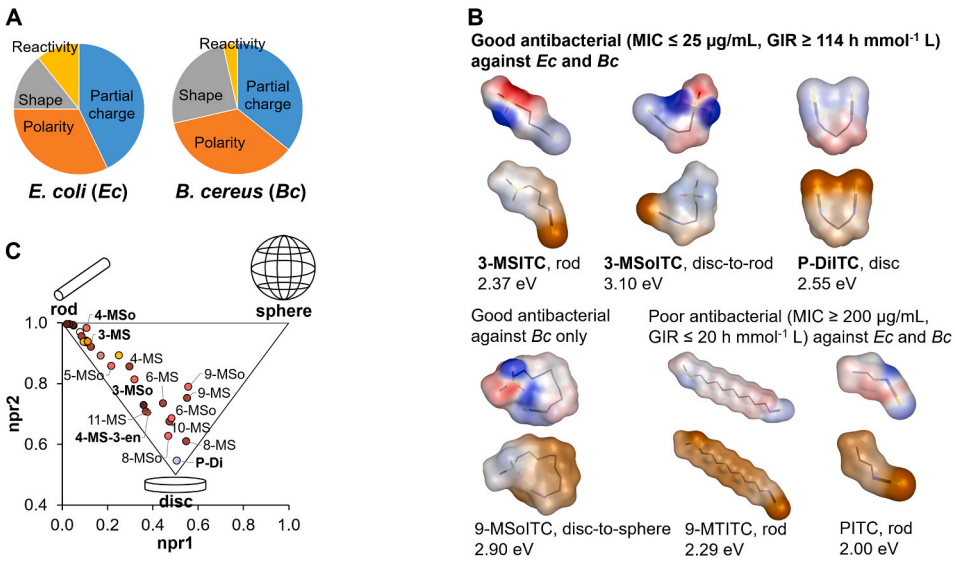

Fig. 4. Important physicochemical properties of ITCs for imparting their antimicrobial activity. Frequency of descriptors related to a physicochemical property (partial charge, polarity, molecular shape, or reactivity) used in the models with 2–5 descriptors for *E. coli* (left) and *B. cereus* (right) (**A**). The physicochemical classification of descriptors is in Table S7. Surface maps of electrostatic regions (blue: partial negative charge; red: partial positive charge) and hydrophobic/hydrophilic regions (yellow: hydrophobic; light blue: hydrophilic) of some representative ITCs (**B**). 3-MSITC: 3-(methylsulfinyl)propyl ITC; 3-MSoITC: 3-(methylsulfonyl)propyl ITC; P-DiITC: 1,3-propylene diisothiocyanate; 9-MSoITC: 9-(methylsulfonyl)nonyl ITC; 9-MTITC: 9-(methylthio)nonyl ITC; PITC: propyl ITC. The numbers (1 eV = 96.5 kJ/mol) underneath the names of ITCs represent the *AM1_Electrophilicity* values. Molecular shape distribution of ITCs in the triangular npr (normalized PMI – principal moment of inertia – ratios) shape space according to (Sauer & Schwarz, 2003) and (Wirth et al., 2013) (**C**). Different subclasses of ITCs are indicated by different colors according to those in Fig. 1. The names of ITCs are represented as the abbreviation of their side chain. ITCs in bold face were good antibacterials (GIR ≥ 114 h mmol^{-1} L, MIC ≤ 25 μg/mL) against both *E. coli* and *B. cereus*, whereas ITCs in light face were good antibacterials only against *B. cereus*. (For interpretation of the references to color in this figure legend, the reader is referred to the Web version of this article.)

(Fig. 4B, orange-light blue surface). The shorter the chain length, the more distinct the hydrophilic and hydrophobic regions (e.g. 3-MSoITC vs 9-MSoITC). In our study, only ITCs with more distinctive hydrophilic and hydrophobic regions exerted activity against both Gram$^-$ *E. coli* and Gram$^+$ *B. cereus*. ITCs with evenly distributed hydrophobicity (e.g. 9-MTITC, PITC) showed poor antibacterial activity against both bacteria.

Polarity related descriptors have been frequently used in QSAR models for other classes of antimicrobial compounds (Araya-Cloutier et al., 2018; de Bruijn et al., 2018). Moreover, our QSAR models for *B. cereus* agree with QSAR models of natural and synthetic 1,4-benzoxazine-3-ones for Gram$^+$ bacteria, in which hydrophilic integy moment and hydrophilic volume descriptors were important (de Bruijn et al., 2018). Polarity as a main physicochemical property for antimicrobial compounds often links to the polarity of microbial cell envelope components, important for uptake of molecules (Richter et al., 2017). High polarity is desirable for good antibacterials against Gram$^-$ *E. coli*, reflected by *TPSA* (p-value 5.7×10^{-10}) and *vsurf_W1* (p-value 3.8×10^{-4}) (Figure S8). The nonspecific porins in the outer membrane of Gram$^-$ bacteria allow small (<600 Da) and hydrophilic antimicrobial molecules to pass (Nikaido, 2003; Richter et al., 2017; Ziervogel & Roux, 2013). As in our study short-chained ITCs with sulfinyl and sulfonyl groups had good activity against *E. coli*, whereas long-chained analogues did not, we suggest that the entry pathway of ITCs into Gram$^-$ *E. coli* cells is via the nonspecific porins. Further studies are required to confirm this hypothesis by using *E. coli* mutant strains lacking of the nonspecific porins (Huang & Hancock, 1996; Mortimer & Piddok, 1993). In contrast, the long-chained analogues were good antibacterials against *B. cereus*. This might be related to the cell envelope of Gram$^+$ bacteria, which generally has less restriction for influx of molecules in comparison to the cell envelope of Gram$^-$ bacteria, characterized by impermeable lipopolysaccharides (Denyer & Maillard, 2002).

4.1.3. The importance of molecular shape

In our models, the shape descriptors *npr1* and *npr2* were correlated to the activity against *B. cereus* and *E. coli*, respectively. The combinatorial *npr1* and *npr2* descriptor values reflect the shape of a molecule (rod, sphere, or disc) (Fig. 4C) (Sauer & Schwarz, 2003; Wirth et al., 2013). For good activity against *E. coli*, ITCs with rod-like shapes are desirable (Fig. 4B–C), except for P-DiITC (disc-like). For good activity against *B. cereus*, ITCs with disc- or rod-like shapes are desirable. This finding agrees with a previous QSAR study of antimicrobial 1,4-benzoxazin-3-ones, where rod-like rather than sphere-like shape was desirable for activity against Gram$^-$ bacteria, and disc- or rod-like shape was desirable for activity against Gram$^+$ bacteria (de Bruijn et al., 2018). Furthermore, another previous study on small antimicrobial molecules (both natural and synthetic derivatives of various classes) indicated that low globularity, i.e. less spherical, was desirable for activity against Gram$^-$ bacteria (Richter et al., 2017).

4.1.4. The importance of reactivity

The reactivity of ITCs is due to the electrophilic carbon of the –N=C=S group. The electrophilic carbon is suggested to be essential for antimicrobial activity of ITCs because of its capability of impairing functions of proteins essential for cell growth and metabolism by forming covalent linkage to nucleophilic groups (particularly thiol, –SH) in the active site of proteins (Dufour, Stahl, & Baysse, 2015). The substituent in the side chain seems to affect the electrophilicity (ω^o, eV) of ITCs more than the chain length does (e.g. 3-MSITC, 2.37 eV; 3-MSoITC, 3.10 eV; 9-MSoITC, 2.90 eV). This is also found for benzenic ITCs (*p*-MSoPhITC, 3.62 eV; BITC, 2.52 eV; PhEITC, 2.48 eV). It is worth to note that electrophilicity alone does not explain the antibacterial activity of ITCs, as the QSAR highlighted, there are other ITCs' physicochemical properties important for imparting the activity. In this respect, *p*-MSoPhITC was the most electrophilic among the 26 ITCs, but was not active against either bacteria. With our current dataset, there seems to be an optimum electrophilicity for an ITC to be a good antibacterial, i.e. 2.3–3.1 eV against *E. coli* and 1.9–3.1 eV against *B. cereus*.

4.2. The bifunctional ITC

P-DiITC had remarkable antimicrobial activity against both bacteria (MIC 6.3–9.4 μg/mL, 0.04–0.06 mmol/L), much higher than that of the monofunctional analogue (PITC, MIC > 200.0 μg/mL, > 1.98 mmol/L). A previous study showed that bifunctional ITC groups improved the activity against Gram$^+$ *B. cereus* (e.g. for two identical compounds except for the number of ITC groups, MIC_{bi} 0.5 μg/mL, MIC_{mono} 16 μg/mL) and against

Gram$^-$ *E. coli* (MIC_{bi} 8 μg/mL, MIC_{mono} 64 μg/mL) (Kurepina, Kreiswirth, & Mustaev, 2013). The enhanced antimicrobial activity of P-DiITC can be explained by twice higher topological polar surface area compared to PITC (Figure S8A) and the two electrophilic sites for the nucleophilic attack.

4.3. Prospects

The antimicrobial activity of *B. oleracea* ITC-rich extract is promising as it has activity against both Gram$^-$ *E. coli* and Gram$^+$ *B. cereus* with MIC 750–1000 μg/mL, whereas other natural extracts, e.g. from rosemary, clove, are often effective only against Gram$^+$ bacteria or require higher concentrations (2500–10,000 μg/mL) to be effective against Gram$^-$ bacteria (Gonelimali et al., 2018). The antimicrobial activity of *C. sativa* ITC-rich extract against Gram$^+$ *B. cereus* is also promising (MIC 188 μg/mL) in comparison with other natural extracts (MIC $\geq$ 315 μg/mL) (Araya-Cloutier, den Besten, Aisyah, Gruppen, & Vincken, 2017; Gonelimali et al., 2018).

The application of ITCs in food products needs further investigation on their pungency, toxicity, and reactivity (Bell, Oloyede, Lignou, Wagstaff, & Methven, 2018). A previous study indicated that the receptor responsible for pungency was *in vitro* activated by alkenyl ITCs, MTITCs, and benzenic ITCs within the concentrations applied in the antimicrobial assay (Terada, Masuda, & Watanabe, 2015). Meanwhile, related information on the most antimicrobial active MSITCs and MSoITCs is still lacking. The toxicity of ITCs seemed to be structure-dependent; the toxic dose of 4-MSITC was 16× higher than that of AITC (EFSA Panel on Food Additives and Nutrient Sources added to Food ANS, 2010; Socała, Nieoczym, Kowalczuk-Vasilev, Wyska, & Wlaź, 2017). Systematic studies on the toxicity of ITCs from different subclasses and chain length need to be done. Due to electrophilicity of ITCs, their antimicrobial activity can also be affected by the nucleophile content present in the growth media or food matrices (Andini, Araya-Cloutier, Waardenburg, et al., 2020).

5. Conclusions

This study was the first QSAR study of ITCs as antibacterials ($n = 26$) covering aliphatic and benzenic ITCs from 9 subclasses against Gram$^-$ and Gram$^+$ bacteria. Models built using p'GIR are recommended for future studies on antimicrobials as it allows the inclusion of compounds with no defined MIC to the QSAR modeling. The developed QSAR models were able to predict the antibacterial activity of ITC-rich extracts well, with one of the extracts containing high abundance of ITCs which were not in the training set. This indicates that the models can potentially be used to predict the activity of (natural) mixtures of ITCs. Overall, MSITCs and MSoITCs are promising antimicrobial candidates to meet the consumers' demand for natural food preservatives and worth further studies.

CRediT authorship contribution statement

Silvia Andini: Conceptualization, Formal analysis, Funding acquisition, Investigation, Validation, Writing – original draft. **Carla Araya-Cloutier:** Writing – review & editing, Supervision. **Bianca Lay:** Investigation, Writing – review & editing. **Gijs Vreeke:** Conceptualization, Investigation, Writing – review & editing. **Jos Hageman:** Data curation, Formal analysis, Methodology, Software, Validation. **Jean-Paul Vincken:** Conceptualization, Funding acquisition, Resources, Writing – review & editing, Supervision.

Declaration of competing interest

The authors declare that they have no known competing financial interests or personal relationships that could have appeared to influence the work reported in this paper.

Acknowledgement

The authors are grateful to Indonesia Endowment Fund for Education (LPDP), Ministry of Finance of Republic Indonesia, to financially support PhD study of SA.

Appendix A. Supplementary data

Supplementary data to this article can be found online at https://doi.org/10.1016/j.lwt.2021.111222.

References

Andini, S., Araya-Cloutier, C., Sanders, M., & Vincken, J.-P. (2020). Simultaneous analysis of glucosinolates and isothiocyanates by RP-UHPLC-ESI-MS^n. *Journal of Agricultural and Food Chemistry, 68*(10), 3121–3131. https://doi.org/10.1021/acs.jafc.9b07920

Andini, S., Araya-Cloutier, C., Waardenburg, L., den Besten, H. M. W., & Vincken, J.-P. (2020). The interplay between antimicrobial activity and reactivity of isothiocyanates. *Lebensmittel-Wissenschaft und -Technologie- Food Science and Technology, 134*, 109843. https://doi.org/10.1016/j.lwt.2020.109843

Andini, S., Dekker, P., Gruppen, H., Araya-Cloutier, C., & Vincken, J.-P. (2019). Modulation of glucosinolate composition in Brassicaceae seeds by germination and fungal elicitation. *Journal of Agricultural and Food Chemistry, 67*(46), 12770–12779. https://doi.org/10.1021/acs.jafc.9b05771

Araya-Cloutier, C., den Besten, H. M. W., Aisyah, S., Gruppen, H., & Vincken, J.-P. (2017). The position of prenylation of isoflavonoids and stilbenoids from legumes (Fabaceae) modulates the antimicrobial activity against Gram positive pathogens. *Food Chemistry, 226*, 193–201. https://doi.org/10.1016/j.foodchem.2017.01.026

Araya-Cloutier, C., Vincken, J.-P., van de Schans, M. G. M., Hageman, J., Schaftenaar, G., den Besten, H. M. W., et al. (2018). QSAR-based molecular signatures of prenylated (iso)flavonoids underlying antimicrobial potency against and membrane-disruption in Gram positive and Gram negative bacteria. *Scientific Reports, 8*(1), 9267. https://doi.org/10.1038/s41598-018-27545-4

Aryani, D. C., den Besten, H. M. W., Hazeleger, W. C., & Zwietering, M. H. (2015). Quantifying strain variability in modeling growth of *Listeria monocytogenes*. *International Journal of Food Microbiology, 208*, 19–29. https://doi.org/10.1016/j.ijfoodmicro.2015.05.006

Bell, L., Oloyede, O. O., Lignou, S., Wagstaff, C., & Methven, L. (2018). Taste and flavor perceptions of glucosinolates, isothiocyanates, and related compounds. *Molecular Nutrition & Food Research, 62*(18), Article e1700990. https://doi.org/10.1002/mnfr.201700990

Blažević, I., Montaut, S., Burčul, F., Olsen, C. E., Burow, M., Rollin, P., et al. (2020). Glucosinolate structural diversity, identification, chemical synthesis and metabolism in plants. *Phytochemistry, 169*, 112100. https://doi.org/10.1016/j.phytochem.2019.112100

de Bruijn, W. J. C., Hageman, J. A., Araya-Cloutier, C., Gruppen, H., & Vincken, J.-P. (2018). QSAR of 1,4-benzoxazin-3-one antimicrobials and their drug design perspectives. *Bioorganic & Medicinal Chemistry, 26*(23), 6105–6114. https://doi.org/10.1016/j.bmc.2018.11.016

Denyer, S. P., & Maillard, J. Y. (2002). Cellular impermeability and uptake of biocides and antibiotics in Gram-negative bacteria. *Journal of Applied Microbiology, 92*(Suppl), 35s–45s. https://doi.org/10.1046/j.1365-2672.92.5s1.19.x|

Dolezal, R., Soukup, O., Malinak, D., Savedra, R. M. L., Marek, J., Dolezalova, M., et al. (2016). Towards understanding the mechanism of action of antibacterial *N*-alkyl-3-hydroxypyridinium salts: Biological activities, molecular modeling and QSAR studies. *European Journal of Medicinal Chemistry, 121*, 699–711. https://doi.org/10.1016/j.ejmech.2016.05.058

Dufour, V., Stahl, M., & Baysse, C. (2015). The antibacterial properties of isothiocyanates. *Microbiology, 161*(Pt 2), 229–243. https://doi.org/10.1099/mic.0.082362-0

Gindulyte, A., Shoemaker, B. A., Yu, B., Fu, G., He, J., Zhang, J., et al. (2015). PubChem substance and compound databases. *Nucleic Acids Research, 44*(D1), D1202–D1213. https://doi.org/10.1093/nar/gkv951

Gonelimali, F. D., Lin, J., Miao, W., Xuan, J., Charles, F., Chen, M., et al. (2018). Antimicrobial properties and mechanism of action of some plant extracts against food pathogens and spoilage microorganisms. [Original Research]. *Frontiers in Microbiology, 9*(1639). https://doi.org/10.3389/fmicb.2018.01639

Gramatica, P. (2007). Principles of QSAR models validation: Internal and external. *QSAR & Combinatorial Science, 26*(5), 694–701. https://doi.org/10.1002/qsar.200610151

Gramatica, P. (2013). On the development and validation of QSAR models. *Methods in Molecular Biology, 930*, 499–526. https://doi.org/10.1007/978-1-62703-059-5_21

Hageman, J. A., Engel, B., de Vos, R. C. H., Mumm, R., Hall, R. D., Jwanro, H., et al. (2017). Robust and confident predictor selection in metabolomics. In S. Datta, & B. J. A. Mertens (Eds.), *Statistical analysis of proteomics, metabolomics, and lipidomics data using mass spectrometry* (pp. 239–257). Cham: Springer International Publishing.

Hawkins, D. M. (2004). The problem of overfitting. *Journal of Chemical Information and Computer Sciences, 44*(1), 1–12. https://doi.org/10.1021/ci0342472

Huang, H., & Hancock, R. E. (1996). The role of specific surface loop regions in determining the function of the imipenem-specific pore protein OprD of *Pseudomonas aeruginosa*. *Journal of Bacteriology, 178*(11), 3085–3090. https://doi.org/10.1128/jb.178.11.3085-3090.1996

Kurepina, N., Kreiswirth, B. N., & Mustaev, A. (2013). Growth-inhibitory activity of natural and synthetic isothiocyanates against representative human microbial pathogens. *Journal of Applied Microbiology, 115*(4), 943–954. https://doi.org/10.1111/jam.12288

Lambert, P. A. (2002). Cellular impermeability and uptake of biocides and antibiotics in Gram-positive bacteria and mycobacteria. *Journal of Applied Microbiology, 92*(s1), 46S–54S. https://doi.org/10.1046/j.1365-2672.92.5s1.7.x

Mortimer, P. G. S., & Piddok, L. J. V. (1993). The accumulation of five antibacterial agents in porin-deficient mutants of *Escherichia coli*. *Journal of Antimicrobial Chemotherapy, 32*(2), 195–213. https://doi.org/10.1093/jac/32.2.195

Nikaido, H. (2003). Molecular basis of bacterial outer membrane permeability revisited. *Microbiology and Molecular Biology Reviews, 67*(4), 593–656. https://doi.org/10.1128/mmbr.67.4.593-656.2003

Parr, R. G., Szentpály, L.v., & Liu, S. (1999). Electrophilicity index. *Journal of the American Chemical Society, 121*(9), 1922–1924. https://doi.org/10.1021/ja983494x

Richter, M. F., Drown, B. S., Riley, A. P., Garcia, A., Shirai, T., Svec, R. L., et al. (2017). Predictive compound accumulation rules yield a broad-spectrum antibiotic. *Nature, 545*(7654), 299–304. https://doi.org/10.1038/nature22308

Roy, K., Chakraborty, P., Mitra, I., Ojha, P. K., Kar, S., & Das, R. N. (2013). Some case studies on application of "r^2m" metrics for judging quality of quantitative structure–activity relationship predictions: Emphasis on scaling of response data. *Journal of Computational Chemistry, 34*(12), 1071–1082. https://doi.org/10.1002/jcc.23231

Sauer, W. H. B., & Schwarz, M. K. (2003). Molecular shape diversity of combinatorial libraries: A prerequisite for broad bioactivity. *Journal of Chemical Information and Computer Sciences, 43*(3), 987–1003. https://doi.org/10.1021/ci025599w

EFSA Panel on Food Additives and Nutrient Sources added to Food (ANS). (2010). Scientific Opinion on the safety of allyl isothiocyanate for the proposed uses as a food additive. *EFSA Journal, 8*, 1943–1983. https://doi.org/10.2903/j.efsa.2010.1943, 12th ed.

Socała, K., Nieoczym, D., Kowalczuk-Vasilev, E., Wyska, E., & Wlaź, P. (2017). Increased seizure susceptibility and other toxicity symptoms following acute sulforaphane treatment in mice. *Toxicology and Applied Pharmacology, 326*, 43–53. https://doi.org/10.1016/j.taap.2017.04.010

Terada, Y., Masuda, H., & Watanabe, T. (2015). Structure-activity relationship study on isothiocyanates: Comparison of TRPA1-activating ability between allyl isothiocyanate and specific flavor components of wasabi, horseradish, and white mustard. *Journal of Natural Products, 78*(8), 1937–1941. https://doi.org/10.1021/acs.jnatprod.5b00272

Tropsha, A. (2010). Best practices for QSAR model development, validation, and exploitation. *Molecular Informatics, 29*(6-7), 476–488. https://doi.org/10.1002/minf.201000061

Tsou, S. H., Hu, S. W., Yang, J. J., Yan, M., & Lin, Y. Y. (2019). Potential oral health care agent from coffee against virulence factor of periodontitis. *Nutrients, 11*(9). https://doi.org/10.3390/nu11092235

Windels, E. M., Michiels, J. E., Fauvart, M., Wenseleers, T., Van den Bergh, B., & Michiels, J. (2019). Bacterial persistence promotes the evolution of antibiotic resistance by increasing survival and mutation rates. *The ISME Journal, 13*(5), 1239–1251. https://doi.org/10.1038/s41396-019-0344-9

Wirth, M., Volkamer, A., Zoete, V., Rippmann, F., Michielin, O., Rarey, M., et al. (2013). Protein pocket and ligand shape comparison and its application in virtual screening. [journal article]. *Journal of Computer-Aided Molecular Design, 27*(6), 511–524. https://doi.org/10.1007/s10822-013-9659-1

Xu, L., & Zhang, W.-J. (2001). Comparison of different methods for variable selection. *Analytica Chimica Acta, 446*(1), 475–481. https://doi.org/10.1016/S0003-2670(01)01271-5

Ziervogel, B. K., & Roux, B. (2013). The binding of antibiotics in OmpF porin. *Structure, 21*(1), 76–87. https://doi.org/10.1016/j.str.2012.10.014